Bioorganic & Medicinal Chemistry 18 (2010) 2777–2784

Contents lists available at ScienceDirect

Bioorganic & Medicinal Chemistry

journal homepage: www.elsevier.com/locate/bmc

Synthesis and evaluation of novel benzothiazole derivatives based on the bithiophene structure as potential radiotracers for β-amyloid plaques in Alzheimer's disease

Meng-Chao Cui, Zi-Jing Li, Rui-Kun Tang, Bo-Li Liu *

Key Laboratory of Radiopharmaceuticals, Ministry of Education, College of Chemistry, Beijing Normal University, Beijing 100875, PR China

ARTICLE INFO

Article history:
Received 10 December 2009
Revised 1 February 2010
Accepted 2 February 2010
Available online 6 February 2010

Keywords:
Alzheimer's disease
β-Amyloid
Imaging agent
Binding assay
Autoradiography

ABSTRACT

In this study, six novel benzothiazole derivatives based on the bithiophene structure were developed as potential β-amyloid probes. In vitro binding studies using Aβ aggregates showed that all of them demonstrated high binding affinities with K_i values ranged from 0.11 to 4.64 nM. In vitro fluorescent staining results showed that these compounds can intensely stained Aβ plaques within brain sections of APP/PS1 transgenic mice, animal model for AD. Two radioiodinated compounds [^{125}I]-2-(5′-iodo-2,2′-bithiophen-5-yl)-6-methoxybenzo[*d*]thiazole [^{125}I]**10** and [^{125}I]-2-(2,2′-bithiophen-5-yl)-6-iodobenzo[*d*]thiazole [^{125}I]**13** were successfully prepared through an iododestannylation reaction. Furthermore, in vitro autoradiography of the AD model mice brain sections showed that both [^{125}I]**10** and [^{125}I]**13** labeled the Aβ plaques specifically with low background. In vivo biodistribution studies in normal mice indicated that [^{125}I]**13** exhibited high brain uptake (3.42% ID/g at 2 min) and rapid clearance from the brain (0.53% ID/g at 60 min), while [^{125}I]**10** showed lower brain uptake (0.87% ID/g at 2 min). In conclusion, these preliminary results of this study suggest that the novel radioiodinated benzothiazole derivative [^{125}I]**13** may be a candidate as an in vivo imaging agent for detecting β-amyloid plaques in the brain of AD patients.

1. Introduction

Alzheimer's disease (AD) is an age-related, irreversible, progressive brain disease which slowly destroys the cognitive functions of the brain by causing memory loss, disorientation and language impairment, etc.[1] Several studies indicate that the accumulation of senile plaques (SPs) composed of misfolded β-amyloid (Aβ) peptides and neurofibrillary tangles (NFTs) made of hyperphosphorylated tau aggregates are two of the pathological hallmarks of AD which begins 10–20 years before any symptoms are obvious.[2–4] Development of imaging probes that target Aβ plaques or neurofibrillary tangles for positron emission tomography (PET) or single photon emission computed tomography (SPECT) will be important for early diagnosis of AD, and it will also provide significant information to evaluate the efficacy of therapies of AD.[5–8]

In the past 10 years a large number of radiolabeled ligands targeting Aβ plaques have been reported. Some of them have so far reached the clinical stage, such as [^{18}F]-2-(1-(2-(*N*-(2-fluoroethyl)-*N*-methylamino)-naphthalene-6-yl)ethylidene)malononitrile ([^{18}F]FDDNP),[9–11] 2-(4′-[^{11}C]methylaminophenyl)-6-hydroxybenzothiazole ([^{11}C]PIB),[12,13] 4-N-[^{11}C]methylamino-4′-hydroxystilbene ([^{11}C]SB-13),[14,15] [^{11}C]-2-(2-[2-dimethylaminothiazol-5-yl]ethenyl)-6-(2-[fluoro]ethoxy)benzoxazole ([^{11}C]BF-227),[16] [^{18}F]-4-(*N*-methylamino)-4′-(2-(2-(2-fluoroethoxy)ethoxy)ethoxy)-stilbene ([^{18}F]BAY 94-9172)[17] for PET imaging (Fig. 1). However, SPECT scanners are widely equipped in hospitals. It is more practical for routine clinical diagnostic. Development of SPECT imaging probes for Aβ plaques will benefit a large number of AD patients. Several groups have reported a lot of radioiodinated ligands for Aβ plaques.[18–20] But most of these ligands had unfavorable in vivo pharmacokinetics which preventing their further development as potential in vivo imaging agents. Up to now, [^{123}I]-6-iodo-2-(4′-dimethylamino-)phenyl-imidazo[1,2]pyridine ([^{123}I]IMPY) is the first SPECT imaging probe tested in human and the results are encouraging.[21–23]

As one of the known Aβ probes, (*E*)-2-((5′-(4-hydroxystyryl)-2,2′-bithiophen-5-yl)methylene)malononitrile (NIAD-4) is a near infrared fluorescent contrast agent for in vivo optical imaging Aβ plaques (Fig. 2). This compound contains a highly hydrophobic bithiophene structure and exhibits high binding affinity to Aβ aggregates (K_i = 10 nM) in the same binding site as ThT. In addition, this agent readily crosses the blood–brain barrier (BBB) and specifically labels the Aβ plaques in the living brain of AD model mice.[24]

Recently, Nilsson and his co-workers identified a class of luminescent conjugated polythiophenes (LCPs) as novel conformation sensitive optical probes for selective staining of protein

* Corresponding author. Tel./fax: +86 010 58808891.
E-mail address: liuboli@bnu.edu.cn (B.-L. Liu).

0968-0896/$ - see front matter © 2010 Elsevier Ltd. All rights reserved.
doi:10.1016/j.bmc.2010.02.002

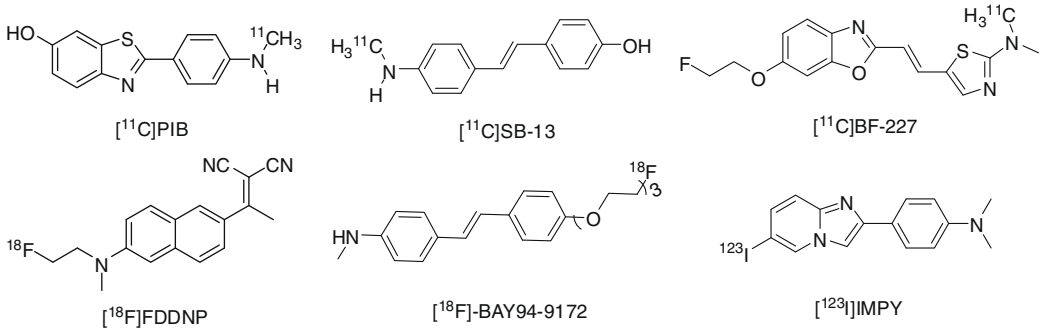

Figure 1. Chemical structure of Aβ imaging probes clinically tested.

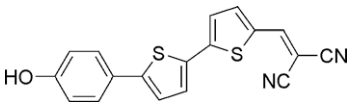

Figure 2. Chemical structure of NIAD-4.

aggregates.[25–27] Under physiological conditions, the pentameric thiophene LCPs showed a striking specificity for both Aβ plaques and NFTs. Two of them also crossed the BBB to a sufficient degree.[28]

Thus, we conclude that the polythiophene moiety may play an important role in maintaining the specific binding ability to Aβ plaques. This prompted us to apply it as a core structure for Aβ imaging agents. Herein we report the synthesis and the initial biological characterizations of the novel benzothiazole derivatives containing the bithiophene structure as probes for Aβ plaques in the brain. To our knowledge, this is the first time bithiophene structures have been introduced to radiotracers for β-amyloid plaques in AD.

2. Results and discussion

2.1. Chemistry

The benzothiazole derivatives (**6–10**) were prepared by a condensation reaction with the chemical yields ranged from 42.5% to 66.3% as depicted in Scheme 1. The 5-substituted-o-aminothiophenols (**1**, **2**) and 5′-substituted-2,2′-bithiophene-5-carbaldehyde (**3–5**) were prepared according to the reported procedures.[29,30] The tributyltin precursors (**11**, **12**) were prepared from the corresponding bromo compounds (**7**, **9**) under a bromo to tributyltin exchange reaction catalyzed by $Pd(PPh_3)_4$ with yields of 14.7%, 21.7%, respectively. The tributyltin derivatives can be readily used as starting materials for preparing [^{125}I]**10** and [^{125}I]**13**. Moreover, the tributyltin precursor **11** was also served as an intermediate in iododestannylation reaction to produce the corresponding iodinated compound **13** with the yield of 30.2%.

2.2. Radiolabeling

The two radioiodinated ligands [^{125}I]**10** and [^{125}I]**13** were prepared from the corresponding tributyltin precursors through an iododestannylation reaction using hydrogen peroxide as oxidant with the radiochemical yields of 53.7% and 66.3%, respectively (Scheme 2). After purification by HPLC, the radio-chemical purities of [^{125}I]**10** and [^{125}I]**13** were both greater than 98%. The specific activity of the no-carrier-added preparation was comparable to that of Na^{125}I, 2200 Ci/mmol. Finally, the radiochemical identities of the radioiodinated ligands were verified by co-injection with nonradioactive compounds by HPLC profiles (Fig. 3).

2.3. Biological studies

2.3.1. Binding assays using the aggregated Aβ(1–40) or Aβ(1–42) peptide in solution

[^{125}I]-4-(6-Iodobenzo[*d*]thiazol-2-yl)-*N*,*N*-dimethylaniline ([^{125}I]-TZDM) was reported to be a selective ligand for in vitro binding of

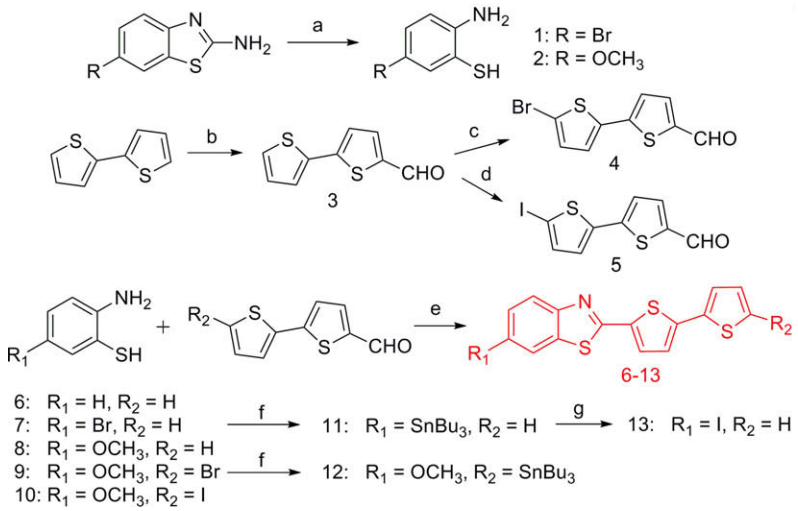

Scheme 1. Reagents and conditions: (a) KOH, H_2O, reflux; (b) $POCl_3$, DMF, 60 °C; (c) AcOH, Br_2; (d) HgO, I_2, toluene; (e) DMSO, 160 °C; (f) $(Bu_3Sn)_2$, $(Ph_3P)_4Pd$, toluene, reflux; (g) I_2, $CHCl_3$.

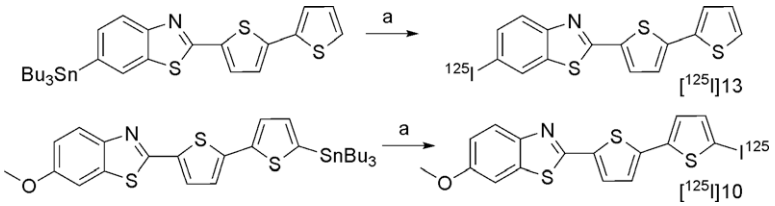

Scheme 2. Reagents: (a) [^{125}I]NaI, HCl (1 M), H_2O_2 (3%).

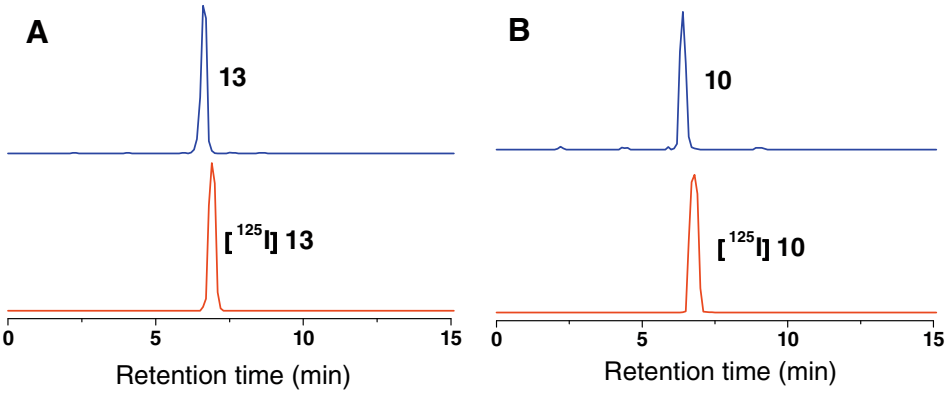

Figure 3. HPLC profiles of **13** (A, top), [^{125}I]**13** (A, bottom) and **10** (B, top), [^{125}I]**10** (B, bottom). HPLC conditions: Agilent TC-C18(2) column (Analytical 4.6 × 150 mm) CH_3CN/H_2O = 9/1, 1 mL/min, 254 nm, **13**t_R (UV) = 6.59 min, [^{125}I]**13**t_R (γ) = 7.00 min and **10**t_R (UV) = 6.38 min, [^{125}I]**10**t_R (γ) = 6.77 min. The slight difference in retention time between the radioactive peak and the UV peak is due to the configuration of the detector system.

Aβ aggregates with high affinities.[18] So the binding affinities of these benzothiazole derivatives were evaluated by inhibition assays against [^{125}I]TZDM using Aβ(1–40) and Aβ(1–42) aggregates as described in the literatures.[18,19,31]

The saturation binding of [^{125}I]TZDM to Aβ(1–40) and Aβ(1–42) showed almost the same K_d values as previously reported [K_d = 0.13 nM for Aβ(1–42), K_d = 0.09 nM for Aβ(1–40), see in Supplementary data]. The K_i values shown in Table 1 suggest that these new compounds share the same binding site as ThT and have excellent binding affinities for both Aβ(1–40) and Aβ(1–42) aggregates. The K_i values of compounds **6**, **7**, **8**, **9**, **10** and **13** were 4.64, 0.60, 2.09, 0.21, 0.11 and 0.25 nM for Aβ(1–40) aggregates and 3.94, 0.57, 0.60, 1.28, 0.61 and 0.31 nM for Aβ(1–42) aggregates, respectively. After analyzing the structures and the corresponding K_i values, we primarily concluded that functional groups may exert moderate effects on the binding affinity. Halogenations at the 5 position (Br or I) on the benzothiazole moiety enhanced the binding affinity (compounds **7** and **13**), while replacing the 5-halogen with a methoxy group also improved the binding affinity (compound **8**). Compounds **9** and **10** with the halogen at 2 position of the bithiophene moiety also displayed high binding affinity. Compared with [^{125}I]TZDM [0.9 nM for Aβ(1–40), 2.2 nM for Aβ(1–42)],[18] [^{11}C]PIB [0.77 nM for Aβ(1–42)][32] and [^{123}I]IMPY [15 nM for Aβ(1–40)],[21] the K_i values of compounds **10** and **13** were superior. In addition, there is no significant difference in the binding affinities between Aβ(1–40) and Aβ(1–42) aggregates.

Table 1
Inhibition constants (K_i) of compounds on ligand binding to aggregates of Aβ(1–40) and Aβ(1–42) versus [^{125}I]TZDM

Compounds	K_i (nM)	
	Aβ(1–42)	Aβ(1–40)
6	3.94 ± 0.06	4.64 ± 0.10
7	0.57 ± 0.08	0.60 ± 0.06
8	0.60 ± 0.06	2.09 ± 0.09
9	1.28 ± 0.08	0.21 ± 0.01
10	0.61 ± 0.09	0.11 ± 0.01
13	0.31 ± 0.05	0.25 ± 0.07
TZDM[a]	2.2 ± 0.4	0.9 ± 0.2
PIB[b]	0.77	—
IMPY[c]	—	15.0 ± 5.0

[a–c] Data from Refs. 18,30,21.

2.3.2. In vitro fluorescent staining of Aβ plaques in transgenic mouse brain sections

Since the in vitro binding assays demonstrated high binding affinities of these compounds for Aβ(1–40) and Aβ(1–42) aggregates, the affinities of compounds **6**, **7**, **8**, **9**, **10** and **13** for Aβ plaques were investigated by neuropathological staining with the brain sections of a 12-month-old transgenic model mouse, Tg-C57, which encoded a double mutant form of APP and PS1. Many Aβ plaques were clearly stained by these compounds with low background (Fig. 4A, C, E, G, I and K). The similar pattern of Aβ plaques was consistent with that stained with thioflavin-S using the adjacent brain section (Fig. 4B, D, F, H, J and L). Such results indicate that these derivatives displayed specific binding affinity for Aβ plaques as supported by the binding assay (Table 1), and may be applied as radiotracers to in vivo amyloid imaging.

2.3.3. In vitro labeling of brain sections from transgenic mouse by autoradiography

To further characterize the specific nature of Aβ plaques binding, in vitro autoradiography was performed by incubating [^{125}I]**10** and [^{125}I]**13**, with the APP/PS1 transgenic mice brain sections in the absence or presence of thioflavin-T (10 mM). Both [^{125}I]**10** and [^{125}I]**13** showed excellent binding to Aβ plaques in the brain sections with a lot of spots of plaque signals in the cortex region and minimal background signals were observed (Fig. 5A and B). The same sections were also stained with thioflavin-S and the localizations of Aβ plaques were accordance with the results of autoradiography (Fig. 5C and D red arrow). In order to confirm that [^{125}I]**10** and [^{125}I]**13** had specific binding to Aβ plaques, blocking

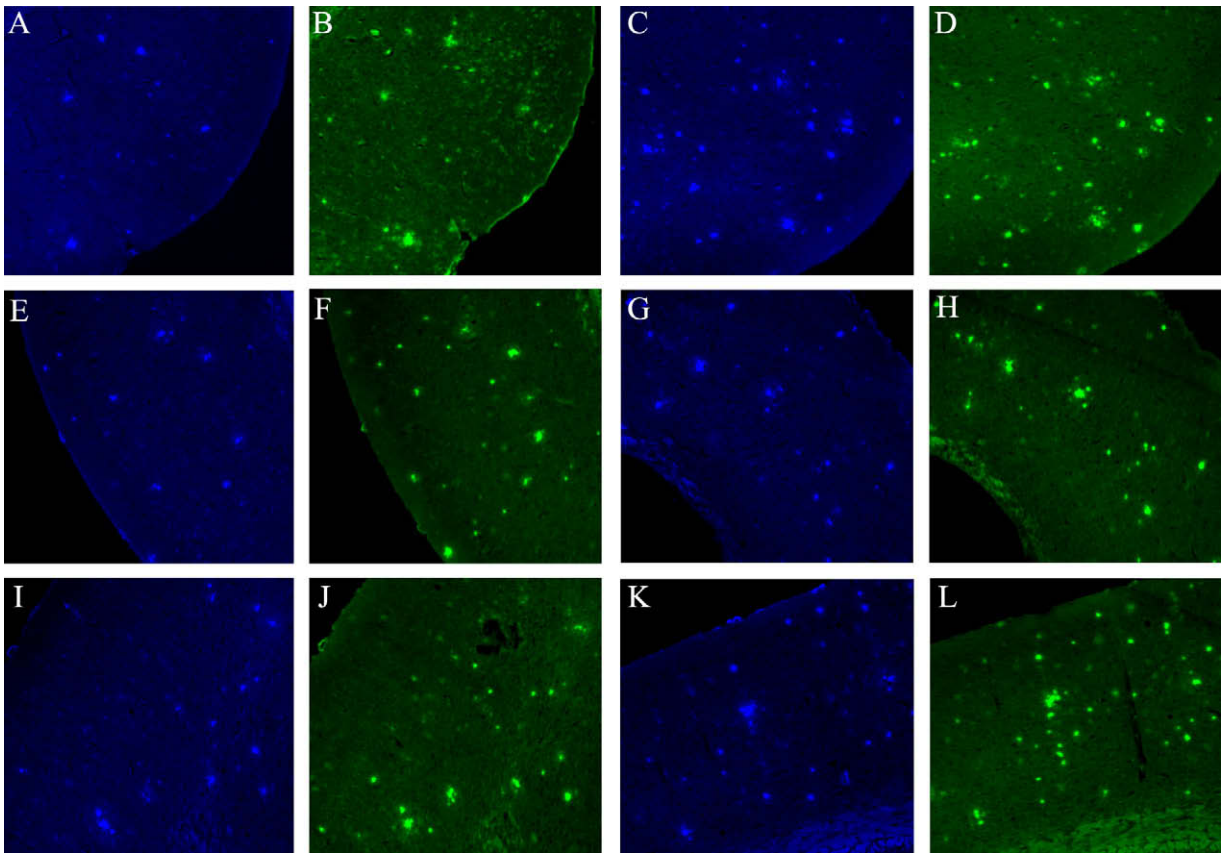

Figure 4. Fluorescence staining of compounds **6**, **7**, **8**, **9**, **10** and **13** (A, C, E, G, I and K) on the sections from a Tg-C57 (APP/PS1) mouse (25 μm thick) with the filter set of DAPI. The labeled plaques were confirmed by staining of the adjacent sections by thioflavin-S (B, D, F, H, J and L) with the filter set of GFP.

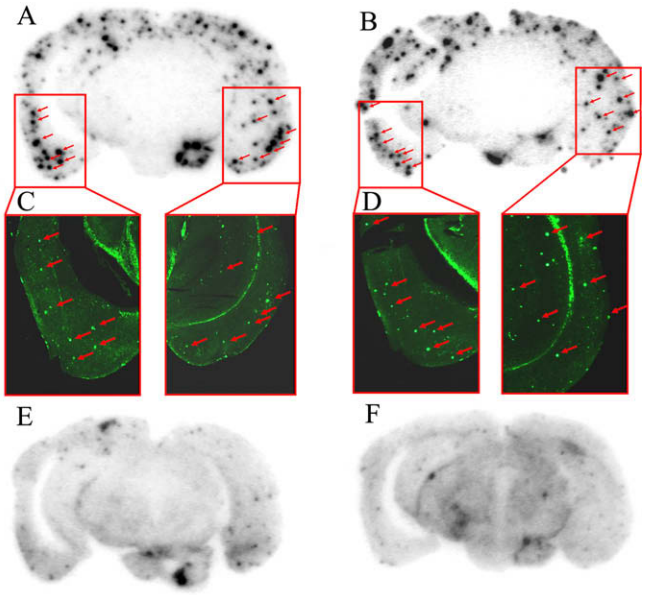

Figure 5. In vitro labeling of brain sections from Tg-C57(APP/PS1) mice (6 μm thick) by autoradiography. [^{125}I]**10** and [^{125}I]**13** strongly labeled the Aβ plaques in the cortex of the brain (A, B). The same sections were also stained with thioflavin-S (C, D) and the localizations of Aβ plaques were accordance with the results of autoradiography (red arrows). The brain sections were pretreated with thioflavin-T (10 mM) (E, F).

study was performed in the presence of thioflavin-T (10 mM) as a blocking agent. The results showed that there was no notable Aβ plaques observed (Fig. 5E and F). In conclusion, [^{125}I]**10** and [^{125}I]**13** were specific for Aβ plaques, which were consistent with the observation that compounds **10** and **13** do bind to Aβ(1–40) and Aβ(1–42) aggregates with high affinity.

2.3.4. In vivo biodistribution in normal mice

The ability to cross the intact BBB is one of the key qualifications for brain imaging agents. The log *D* values of [^{125}I]**10** and [^{125}I]**13** were 3.27, 3.65, respectively (measured by a partition between 1-octanol and pH 7.4 phosphate buffer) which indicate a better BBB penetration. To evaluate brain uptake of the two radioiodinated ligands, [^{125}I]**10** and [^{125}I]**13** were injected intravenously into normal mice for biodistribution experiments. As shown in Table 2, [^{125}I]**13** displayed rapid brain entry at early time intervals. The initial brain uptake was 3.42 ± 0.45% ID/g at 2 min post-injection, which is favorable for potential clinical imaging studies. The brain radioactivity concentration decreased rapidly to 1.08 ± 0.07% ID/g at 30 min and 0.53 ± 0.08% ID/g at 60 min for there is no Aβ plaques in normal mice. These results indicate that [^{125}I]**13** possess favorable pharmacokinetics in brain. However, the initial brain uptake of [^{125}I]**10** was 0.87 ± 0.16% ID/g at 2 min and displayed a slow washout rate from the brain with 0.77 ± 0.16% ID/g at 60 min, which is unfavorable for an Aβ imaging agent.

[^{123}I]IMPY is the most promising SPECT imaging probe which display high binding affinity for Aβ plaques (K_i = 15 nM), excellent brain uptake (2.88% ID/organ at 2 min) and fast washout (0.21% ID/organ at 60 min). In comparison with [^{123}I]IMPY, [^{125}I]**13** displayed superior binding affinity and also illustrated suitable in vivo pharmacokinetic properties for Aβ imaging.

Another noteworthy feature of the radioiodinated imaging agent is the stability in vivo. As shown in Table 2, for both of the

Table 2
Biodistribution in normal mice after iv injection of [^{125}I]**13**, [^{125}I]**10** and the lipophilicity (log *D*) of the ligands[a]

Organ	2 min	30 min	60 min	120 min	240 min
[^{125}I]**13** (log *D* = 3.65 ± 0.04)					
Blood	9.02 ± 2.33	2.12 ± 0.30	1.96 ± 0.16	1.76 ± 0.20	1.36 ± 0.29
Brain	3.42 ± 0.45	1.08 ± 0.07	0.53 ± 0.08	0.51 ± 0.09	0.50 ± 0.11
Heart	4.39 ± 0.72	2.49 ± 0.77	2.65 ± 0.26	1.50 ± 0.21	1.31 ± 0.27
Liver	53.64 ± 5.24	39.81 ± 3.51	29.12 ± 2.24	22.47 ± 4.10	13.82 ± 1.43
Spleen	12.75 ± 4.82	6.78 ± 0.89	8.61 ± 2.02	3.50 ± 0.99	2.07 ± 0.57
Lung	17.51 ± 2.44	8.04 ± 0.35	8.01 ± 2.22	5.76 ± 1.35	3.72 ± 0.62
Kidney	4.00 ± 0.29	7.22 ± 0.39	8.52 ± 1.52	7.33 ± 1.59	5.76 ± 1.09
Stomach[b]	0.39 ± 0.09	2.47 ± 0.74	4.05 ± 1.11	4.39 ± 1.25	3.24 ± 1.15
Muscle	0.65 ± 0.14	1.01 ± 0.02	1.47 ± 0.21	1.23 ± 0.27	0.87 ± 0.15
[^{125}I]**10** (log *D* = 3.27 ± 0.01)					
Blood	23.34 ± 2.79	6.55 ± 0.34	6.58 ± 0.54	6.62 ± 1.19	5.05 ± 0.73
Brain	0.87 ± 0.16	0.64 ± 0.09	0.77 ± 0.16	0.68 ± 0.11	0.53 ± 0.08
Heart	16.13 ± 2.86	5.94 ± 0.46	4.74 ± 0.83	3.48 ± 1.35	2.50 ± 0.69
Liver	35.25 ± 1.78	6.98 ± 0.51	5.76 ± 0.56	4.33 ± 0.83	3.23 ± 0.37
Spleen	19.04 ± 3.73	7.11 ± 0.83	6.24 ± 0.71	4.92 ± 0.80	4.49 ± 0.91
Lung	43.6 ± 2.51	10.28 ± 1.13	8.64 ± 0.75	7.7 ± 1.02	6.12 ± 1.12
Kidney	14.3 ± 1.09	6.49 ± 0.61	6.28 ± 0.67	5.67 ± 1.15	4.53 ± 0.58
Stomach[b]	1.31 ± 0.22	15.84 ± 2.80	20.24 ± 1.57	33.95 ± 5.73	19.37 ± 3.31
Muscle	2.73 ± 0.44	3.42 ± 0.18	3.56 ± 0.30	2.46 ± 0.60	1.95 ± 0.38

[a] Expressed as % injected dose per gram. Average of 5 mice ± standard deviation.
[b] Expressed as % injected dose per organ.

radioiodinated ligands [^{125}I]**10** and [^{125}I]**13**, accumulations of radioactivity in stomach were low, 1.31 ± 0.22% ID/organ and 0.39 ± 0.09% ID/organ at 2 min, however [^{125}I]**10** exhibited a significant increase to 20.24 ± 1.57% ID/organ at 1 hour and 33.95 ± 5.73% ID/organ at 2 hours. This observation demonstrated that [^{125}I]**10** is not stable in vivo, which may result from deiodination caused by oxidation of the sulfur atom in a metabolically active organ.[33] To further illustrate this observation, we performed the stability study of [^{125}I]**10** in plasma and liver homogenate from mouse. The results indicate that [^{125}I]**10** is very stable in plasma, for two hours it does not show any decomposition (Fig. 6E). But in liver homogenate, [^{125}I]**10** quickly deiodinated. After two hours incubation, about 71% of [^{125}I]**10** transformed to free iodine (Fig. 6J). From several published articles, the uptake of free iodine in the glandular stomach was described for mice, rats, hamsters and cats.[34–36] So we can conclude that [^{125}I]**10** first undergoes a deiodination process in liver then accumulated in stomach.

3. Conclusions

In conclusion, we successfully designed and synthesized a series of novel benzothiazole derivatives containing the bithiophene moiety as Aβ imaging agents. These derivatives displayed high in vitro binding affinities for Aβ aggregates. When labeled with ^{125}I, [^{125}I]**10** and [^{125}I]**13** showed specific labeling of Aβ plaques in the brain sections of AD model mice. In addition, [^{125}I]**13** displayed

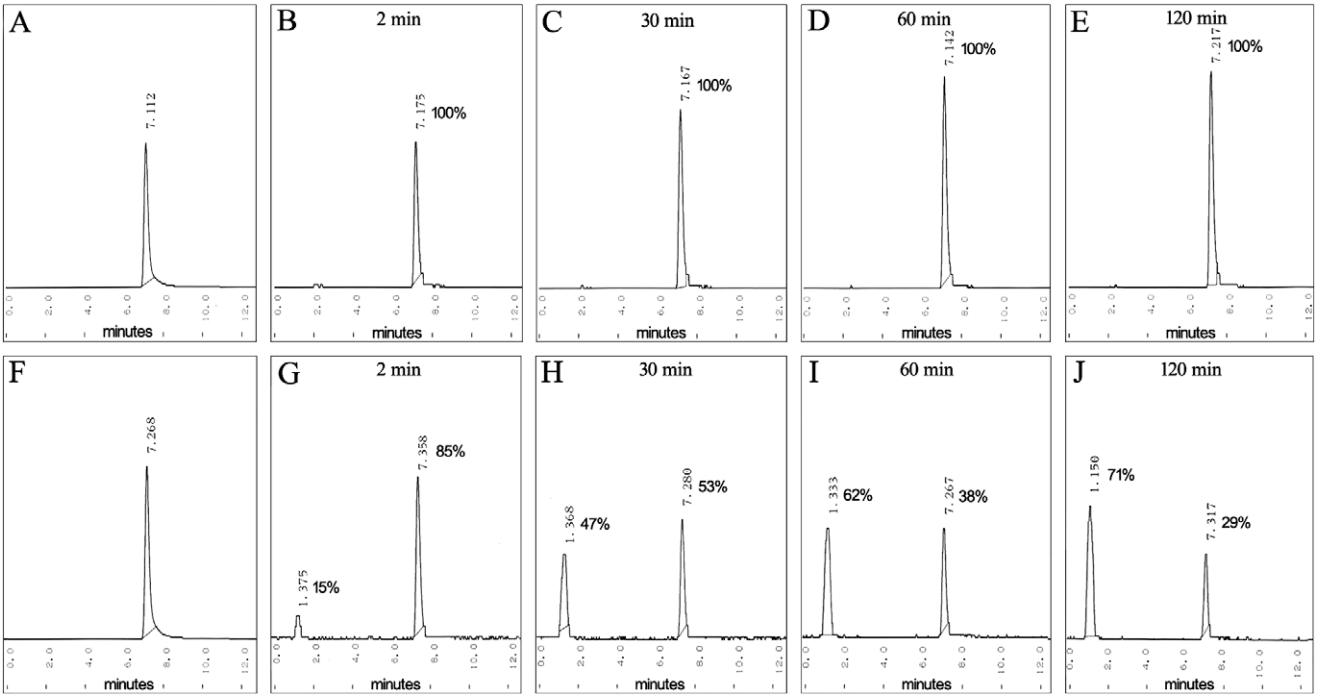

Figure 6. HPLC profiles of [^{125}I]**10** in 10% ethanol (A, F), and after incubation in mice plasma (B–E) and liver homogenate (G–J) at 37 °C for 2 min, 30 min, 1 h and 2 h.

excellent brain uptake and rapid washout from the brain after injection in normal mice. Taken together, [^{125}I]**13** may be a promising candidate Aβ imaging agent for SPECT.

4. Experimental section

4.1. General information

All chemicals used in synthesis were commercial products and were used without further purification unless otherwise indicated. Na^{125}I (2200 Ci/mmol) was obtained from PerkinElmer Life and Analytical Sciences, USA. The double transgenic (APP/PS1) AD model mouse was obtained from Institute of Laboratory Animal Science, Chinese Academy of Medical Sciences and Comparative Medicine Center of Peking Union Medical College, China. ^{1}H NMR spectra were obtained at 400 MHz on Bruker NMR spectrometers in $CDCl_3$ solution at room temperature with TMS as an internal standard. Chemical shifts are reported as δ values relative to internal TMS. Coupling constants are reported in hertz. The multiplicity is defined by s (singlet), d (doublet), t (triplet), and m (multiplet). Mass spectra were acquired under SurveyorMSQ Plus (ESI) instrument. Elemental analyses were obtained on a Elementar Vario EI. HPLC analysis was performed on a Shimadzu SCL-10 AVP equipped with a Packard 500 TR series flow scintillation analyzer, conditions: Agilent TC-C18 reverse-phase analytical column (5 μ, ID = 4.6 mm, length = 150 mm), 90:10 CH_3CN/H_2O, 1.0 mL/min, UV 254 nm. Separations were achieved on a Alltech HPLC pump Model 626 equipped with LINEAR UVIS-201 and BIOSCAN flow-counter, conditions: Alltech C18 reverse-phase column (5 μ, ID = 4.6 mm, length = 250 mm) eluted with acetonitrile at a 2.0 mL/min flow rate.

4.2. Synthesis of 2-amino-5-bromobenzenethiol (1)

2-Amino-5-bromobenzenethiol was synthesized according to the literature.[29] Briefly 2-amino-5-bromobenzothiazole (9.16 g, 40 mmol) was suspended in 50% KOH (80 g KOH dissolved in 80 mL water). The suspension was heated to reflux for 24 h, and was cooled to room temperature. After that, the residue was filtered and the filtrate was neutralized with acetic acid (30% in water, 100 mL) to give the crude product which was used without further purification (66.7% yield).

4.3. Synthesis of 2-amino-5-methoxybenzenethiol (2)

The same reaction as described above for preparing **1** was employed, and a yellow solid **2** was obtained (51.3% yield).

4.4. Synthesis of 2,2′-bithiophene-5-carbaldehyde (3)

According to the literature,[30] $POCl_3$ (2.30 g 15.0 mmol) was added to DMF (1.10 g 15.0 mmol) at 0 °C and the mixture was stirred for 15 min at 0 °C. After that 2,2′-bithiophene (2.00 g 12.0 mmol) dissolved in 1,2-dichloroethane (40 mL) were added dropwise with stirring. The reaction mixture was then heated 2 h at 60 °C. The organic layer was washed with saturated $NaHCO_3$ aqueous solution, and was dried with anhydrous Na_2SO_4. After the solvent was removed, the residue was purified by column chromatography (petroleum ether/AcOEt, 8:1) to give 1.47 g of **3** as a yellow solid (63.1% yield). MS (ESI): *m/z* calcd for $C_9H_6OS_2$ 193.99; found 194.9 ($M+H^+$).

4.5. Synthesis of 5′-bromo-2,2′-bithiophene-5-carbaldehyde (4)

To a stirring solution of 2,2′-bithiophene-5-carboxaldehyde (1.94 g, 10.00 mmol) in $CHCl_3$ (20 mL) at 0 °C, was added bromine (1.60 g, 10.00 mmol) dissolved in $CHCl_3$ (20 mL). The mixture was stirred at room temperature for 2 h. The organic layer was washed with saturated $NaHCO_3$ aqueous solution, and was dried with anhydrous Na_2SO_4. Evaporation of the solvent under reduced pressure gave **4** as a yellow solid (86.3% yield). MS (ESI): *m/z* calcd for $C_9H_5BrOS_2$ 271.90; found 272.9 ($M+H^+$).

4.6. Synthesis of 5′-iodo-2,2′-bithiophene-5-carbaldehyde (5)

To a solution of 2,2′-bithiophene-5-carboxaldehyde (1.94 g, 10.00 mmol) in toluene (20 mL) at 0 °C, was added small portions of mercury(II) oxide (2.23 g, 10.29 mmol, yellow powder) and iodine (2.87 g, 11.32 mmol). The mixture was stirred at room temperature for 8 h, and the orange precipitate was filtered off and washed with ethyl acetate. The filtrate and washings were combined and washed with aqueous sodium thiosulfate and dried over magnesium sulfate. Solvent was removed by rotary evaporation and the solid residue was recrystallized from ethanol to give 2.37 g of **5** (72% yield). MS (ESI): *m/z* calcd for $C_9H_5IOS_2$ 319.88; found 320.8 ($M+H^+$).

4.7. Synthesis of 2-(2,2′-bithiophen-5-yl)benzo[*d*]thiazole (6)

A mixture of 2-aminobenzenethiol (125 mg, 1 mmol) and 2,2′-bithiophene-5-carbaldehyde (194 mg, 1 mmol) in DMSO was heated at 160 °C for 25 min. Ice water (10 mL) was added after the mixture was cooled. The solid was filtered and recrystallized in ethanol to give 168 mg of **6** (56.2% yield). ^{1}H NMR (400 MHz, $CDCl_3$) δ 8.05 (d, J = 8.1 Hz, 1H), 7.86 (d, J = 8.0 Hz, 1H), 7.61 (d, J = 3.7 Hz, 1H), 7.50 (t, J = 7.1 Hz, 1H), 7.39 (t, J = 7.1 Hz, 1H), 7.31 (d, J = 4.4 Hz, 2H), 7.21 (d, J = 3.9 Hz, 1H), 7.08 (t, J = 4.4 Hz, 1H). MS (ESI): *m/z* calcd for $C_{15}H_9NS_3$ 298.99; found 300.3 ($M+H^+$). Anal. Calcd: C, 60.17; H, 3.03; N, 4.68. Found: C, 59.63; H, 3.41; N, 4.72. Mp 165.3–167.0 °C.

4.8. Synthesis of 2-(2,2′-bithiophen-5-yl)-6-bromobenzo[*d*]-thiazole (7)

The same reaction as described above for preparing **6** was employed, a yellow solid **7** was obtained (66.3% yield). ^{1}H NMR (400 MHz, $CDCl_3$) δ 7.98 (d, J = 1.7 Hz, 1H), 7.85 (d, J = 8.7 Hz, 1H), 7.57 (dd, J = 8.7, 1.8 Hz, 1H), 7.54 (d, J = 3.9 Hz, 1H), 7.31 (d, J = 5.4 Hz, 2H), 7.19 (d, J = 3.9 Hz, 1H), 7.07 (t, J = 4.2 Hz, 1H). MS (ESI): *m/z* calcd for $C_{15}H_8BrNS_3$ 376.90; found 378.2 ($M+H^+$). Anal. Calcd: C, 47.62; H, 2.13; N, 3.70. Found: C, 47.56; H, 2.38; N, 3.61. Mp 205.6–207.0 °C.

4.9. Synthesis of 2-(2,2′-bithiophen-5-yl)-6-iodobenzo[*d*]-thiazole (13)

To a solution of **11** (59 mg, 0.1 mmol) in $CHCl_3$ (10 mL) was added a solution of iodine (127 mg dissolved in 10 mL $CHCl_3$) dropwise at room temperature. The resulting mixture was stirred at room temperature for 30 min and quenched by addition of 2 mL saturated $NaHSO_3$ solution. The organic phase was separated, dried over $MgSO_4$, filtered, and concentrated to give the crude product which was recrystallized in AcOEt to give 13 mg of **13** (30.2% yield). ^{1}H NMR (400 MHz, $CDCl_3$) δ 8.18 (s, 1H), 7.77 (s, 2H), 7.64 (d, J = 3.9 Hz, 2H), 7.31–7.32 (m, 2H), 7.20 (d, J = 3.9 Hz, 1H), 7.07 (dd, J = 5.0, 3.9 Hz, 1H). MS (ESI): *m/z* calcd for $C_{15}H_8INS_3$ 424.89; found 425.9 ($M+H^+$). Anal. Calcd: C, 42.36; H, 1.90; N, 3.29. Found: C, 42.31; H, 1.78; N, 3.33. Mp 216.0–217.2 °C.

4.10. Synthesis of 2-(2,2′-bithiophen-5-yl)-6-methoxybenzo[*d*]-thiazole (8)

The same reaction as described above for preparing **6** was employed, and a yellow solid **8** was obtained (42.5% yield). ^{1}H NMR

(400 MHz, $CDCl_3$) δ 7.95 (d, J = 8.9 Hz, 1H), 7.58 (d, J = 3.9 Hz, 1H), 7.31 (dd, J = 6.2, 3.0 Hz, 3H), 7.20 (d, J = 3.9 Hz, 1H), 7.10 (dd, J = 9.0, 2.5 Hz, 1H), 7.07 (d, J = 4.6 Hz, 1H), 3.90 (s, 3H). MS (ESI): m/z calcd for $C_{16}H_{11}NOS_3$ 329.00; found 330.3 ($M+H^+$). Anal. Calcd: C, 58.33; H, 3.37; N, 4.25. Found: C, 58.21; H, 3.69; N, 4.21. Mp 166.6–167.2 °C.

4.11. Synthesis of 2-(5′-bromo-2,2′-bithiophen-5-yl)-6-methoxybenzo[*d*]thiazole (9)

The same reaction as described above for preparing **6** was employed, and a brown solid **9** was obtained (52.1% yield). ^1H NMR (400 MHz, $CDCl_3$) δ 7.94 (d, J = 8.8 Hz, 1H), 7.55 (s, 1H), 7.30 (s, 1H), 7.09 (d, J = 10.5 Hz, 2H), 7.02 (s, 2H), 3.89 (s, 3H). MS (ESI): m/z calcd for $C_{16}H_{10}BrNOS_3$ 406.91; found 408.3 ($M+H^+$). Anal. Calcd: C, 47.06; H, 2.47; N, 3.43. Found: C, 47.16; H, 2.39; N, 3.61. Mp 208.0–209.6 °C.

4.12. Synthesis of 2-(5′-iodo-2,2′-bithiophen-5-yl)-6-methoxybenzo[*d*]thiazole (10)

The same reaction as described above for preparing **6** was employed, and a yellow solid **10** was obtained (47.2% yield). ^1H NMR (400 MHz, $CDCl_3$) δ 7.94 (d, J = 9.0 Hz, 1H), 7.56 (d, J = 3.3 Hz, 1H), 7.31 (s, 1H), 7.20 (d, J = 3.0 Hz, 1H), 7.12 (d, J = 3.0 Hz, 1H), 7.09 (d, J = 8.8 Hz, 1H), 6.95 (s, 1H), 3.90 (s, 3H). MS (ESI): m/z calcd for $C_{16}H_{10}INOS_3$ 454.90 found 456.3 ($M+H^+$). Anal. Calcd: C, 42.20; H, 2.21; N, 3.08. Found: C, 42.27; H, 2.46; N, 2.91. Mp 262.1–263.2 °C.

4.13. Synthesis of 2-(2,2′-bithiophen-5-yl)-6-(tributylstannyl)benzo[*d*]thiazole (11)

A mixture of **7** (189 mg, 0.5 mmol), bis(tributyltin) (580 mg, 1.0 mmol), and $Pd(Ph_3P)_4$ (12.0 mg, 0.01 mmol) in toluene was stirred at 110 °C for 12 h. The solvent was removed, and the residue was purified by column chromatography (petroleum ether/AcOEt, 10:1) to give 86.5 mg of **11** as a yellow solid (14.7% yield). ^1H NMR (400 MHz, $CDCl_3$) δ 7.90 (d, J = 7.9 Hz, 1H), 7.85 (s, 1H), 7.48 (d, J = 3.9 Hz, 1H), 7.46 (d, J = 4.7 Hz, 1H), 7.21 (d, J = 4.4 Hz, 1H), 7.11 (d, J = 3.9 Hz, 1H), 7.00–6.98 (m, 1H), 1.53–1.45 (m, 6H), 1.33–1.23 (m, 6H), 1.07–1.04 (m, 6H), 0.83 (t, J = 8.4 Hz, 9H). MS (ESI): m/z calcd for $C_{27}H_{35}NS_3Sn$ 589.10; found 590.0 ($M+H^+$).

4.14. Synthesis of 6-methoxy-2-(5′-(tributylstannyl)-2,2′-bithiophen-5-yl)benzo[*d*]thiazole (12)

The same reaction as described above for preparing **11** was employed, and a yellow solid **12** was obtained from **9** (21.7% yield). ^1H NMR (400 MHz, $CDCl_3$) δ 7.89 (d, J = 8.9 Hz, 1H), 7.47 (d, J = 3.9 Hz, 1H), 7.39 (d, J = 3.4 Hz, 1H), 7.31 (d, J = 2.5 Hz, 1H), 7.17 (d, J = 3.9 Hz, 1H), 7.10 (d, J = 3.4 Hz, 1H), 7.07 (dd, J = 9.0, 2.6 Hz, 1H), 3.89 (s, 3H), 1.64–1.54 (m, 6H), 1.41–1.31 (m, 6H), 1.17–1.08 (m, 6H), 0.91 (t, J = 7.3 Hz, 9H). MS (ESI): m/z calcd for $C_{28}H_{37}NOS_3Sn$ 619.11; found 620.2 ($M+H^+$).

4.15. Preparation of radioiodinated ligands

The radioiodinated compounds [^{125}I]**10** and [^{125}I]**13** were prepared from the corresponding tributyltin derivatives by an iododestannylation according to the procedure described previously with some modifications. Briefly, 100 μL of H_2O_2 (3%) was added to a mixture of a tributyltin derivative (0.1 mg/100 μL in ethanol), 240 μCi sodium [^{125}I]iodide (specific activity 2200 Ci/mmol), and 100 μL of 1 M HCl in a sealed vial. The reaction was allowed to proceed at room temperature for 15 min and then quenched by addition of 50 μL saturated $NaHSO_3$ solution. The reaction mixture, after neutralization with 1 M NaOH was purified by HPLC on a Alltech C18 reverse-phase column (5 μ, ID = 4.6 mm, length = 250 mm) with the solvent of acetonitrile (100%) at a flow rate of 2.0 mL/min. The desired fractions containing the product were evaporated to dryness and redissolved in 100% ethanol. The final product was stored at −20 °C for in autoradiography and biodistribution studies.

4.16. Binding assays using the aggregated Aβ(1–40) or Aβ(1–42) peptide in solution

The trifluoroacetic acid salt forms of peptides Aβ(1–40) and Aβ(1–42) were purchased from GL biochem (Shanghai, China). Aggregation of peptides was carried out by gently dissolving the peptide [0.25 mg/mL for Aβ(1–40) and Aβ(1–42)] in a buffer solution (pH 7.4) containing 10 mM sodium phosphate and 1 mM EDTA. The solutions were incubated at 37 °C for 42 h with gentle and constant shaking. Inhibition studies were carried out in 12 × 75 mm borosilicate glass tubes according to the procedure described previously with some modifications.[18,31] Fifty microliters of aggregated Aβ fibrils (28 nM in the final assay mixture) were added to the mixture containing 100 μL of radioligands ([^{125}I]TZDM) with appropriate concentration, 10 μL of inhibitors (10^{-5} – 10^{-10} M in ethanol) and 840 μL PBS (0.2 M, pH 7.4) in a final volume of 1 mL. Nonspecific binding was defined in the presence of 100 nM TZDM. The mixture was incubated for 2 h at 37 °C, then the bound and free radioactivities were separated by vacuum filtration through borosilicate glass fiber filters (0.1 μm, JiuDing, China) using a ZT-II cell harvester (Shaoxing, China) followed by 3 × 4 mL washes of cold PBS (0.2 M, pH 7.4) containing 10% ethanol at room temperature. Filters containing the bound ^{125}I ligand were counted in a γ-counter (WALLAC/Wizard 1470, USA) with 71% counting efficiency. Under the assay conditions, the percent of the specifically bound fraction was about 20% of the total radioactivity. The half maximal inhibitory concentration (IC_{50}) values were determined using GraphPad Prism 4.0, and those for the inhibition constant (K_i) were calculated using the Cheng–Prusoff equation: $K_i = IC_{50}/(1 + [L]/K_d)$.[37]

4.17. In vitro fluorescent staining of Aβ plaques in transgenic mouse brain sections

The transgenic model mice, Tg-C57, which encodes a double mutant form of APP and PS1 was used for the studies. Mice were sacrificed by cervical dislocation and brains were rapidly removed and frozen. Coronal 25 μm sections were cut in a Leica-CM1900 cryostat from frozen (−25 °C), unfixed brains, and thaw mounted onto poly-L-lysine coated microscope slides (Ultra-Lab, China). The brain sections were incubated with 10% ethanol solution (100 nM) of **6**, **7**, **8**, **9**, **10** and **13** for 10 min. The localization of plaques was confirmed by staining with thioflavin-S (1 μm) on the adjacent sections. Finally, the sections were washed with 50% ethanol and PBS (0.2 M, pH 7.4) for 10 min. Fluorescent observation was performed by the LSM 510 META (Zeiss, Germany) equipped with DAPI (excitation, 405 nm) and GFP filter sets (excitation, 505 nm).

4.18. In vitro labeling of brain sections from transgenic mouse by autoradiography

Paraffin-embedded brain sections of Tg-C57 mouse (6 μm) which were from Chinese Academy of Medical Sciences were used for the autoradiography. The brain sections were deparaffinized with 2 × 20 min washes in xylene; 2 × 5 min washes in 100% ethanol; 5 min washes in 90% ethanol/H_2O; 5 min washes in 80%

ethanol/H_2O; 5 min wash in 60% ethanol/H_2O; running tap water for 10 min, and then incubated in PBS (0.2 M, pH 7.4) for 30 min. The sections were incubated with [^{125}I]**10** and [^{125}I]**13** in the absence or in the presence of thioflavin-T (10 mM) for 30 min at room temperature. The sections were then washed with saturated Li_2CO_3 in 40% ethanol for 3 min and washed with 40% ethanol for 3 min, followed by rinsing with water for 30 s. After drying, the ^{125}I-labeled sections were exposed to phosphorus film for 2 h then scanned with the phosphor imaging system (Cyclone, Packard) at the resolution of 600 dpi. The presence and localization of plaques were confirmed by the fluorescent staining with thioflavin-S (1 μm) on the same sections using Stereo Discovery V12, excitation: 450–490 nm, emission: 500–550 nm, (Zeiss, Germany).

4.19. In vivo biodistribution in normal mice

In vivo biodistribution Studies were performed in female Kunming normal mice (average weight about 20 g) and was approved by the animal care committee of Beijing Normal University. A saline solution (100 μL) containing [^{125}I]**10** or [^{125}I]**13** (1 μCi) was injected directly into the tail vein of mice. The mice were sacrificed at various time points post-injection. The organs of interest were removed and weighed, and the radioactivity was counted with an automatic γ-counter (WALLAC/Wizard 1470, USA). The percentage dose per gram of wet tissue was calculated by a comparison of the tissue counts to suitably diluted aliquots of the injected material.

4.20. Partition coefficient determination

The determination of partition coefficient of [^{125}I]**10** and [^{125}I]**13** were performed according to the procedure previously reported with some modifications.[38] Five μCi of [^{125}I]**10** or [^{125}I]**13** was added to the premixed suspensions containing 3× of *n*-octanol and 3 g of PBS (0.05 M, pH 7.4) in a test tube. The test tube was vortexed for 3 min at room temperature, followed by centrifugation for 5 min at 3500 rpm. Two weighted samples from the *n*-octanol (50 μL) and buffer (800 μL) layers were counted. The partition coefficient was expressed as the logarithm of the ratio of the counts per gram from *n*-octanol versus that of PBS. Samples from *n*-octanol layer were repartitioned until consistent partitions of coefficient values were obtained. The measurement was done in triplicate and repeated three times.

4.21. Stability study

The stability in mouse plasma and liver homogenate was determined by incubating 10 μCi purified [^{125}I]**10** in the solution of 100 μL mouse plasma or mouse liver homogenate at 37 °C for 2 min, 30 min, 60 min and 120 min. Proteins were precipitated by adding 200 μL acetonitrile, after centrifugation at 5000 rpm for 15 min at −4 °C. The radiochemical purity was analyzed by HPLC.

Acknowledgments

The authors thank Dr. Lianfeng Zhang (Institute of Laboratory Animal Science, Chinese Academy of Medical Sciences and Comparative Medicine Center of Peking Union Medical College) for kindly provided the Paraffin-embedded brain sections of AD model mice, Dr. Hongmei Jia (College of Chemistry, Beijing Normal University) for many thoughtful discussions and preparation of the manuscript and Dr. Xiaoyan Zhang (College of Life Science, Beijing Normal University) for assistance in the in vitro neuropathological staining. The authors also thank Dr. Yan Cheng (Department of Patho-Functional Bioanalysis, Graduate School of Pharmaceutical Sciences, Kyoto University) for her help with preparation of the manuscript. This work was funded by NSFC (20871021).

Supplementary data

Supplementary data associated with this article can be found, in the online version, at doi:10.1016/j.bmc.2010.02.002.

References and notes

1. Hardy, J. A.; Higgins, G. A. *Science* **1992**, *256*, 184.
2. Selkoe, D. J. *JAMA-J. Am. Med. Assoc.* **2000**, *283*, 1615.
3. Hardy, J. A.; Selkoe, D. J. *Science* **2002**, *297*, 353.
4. Selkoe, D. J. *Physiol. Rev.* **2001**, *81*, 741.
5. Mathis, C. A.; Wang, Y.; Klunk, W. E. *Curr. Pharm. Des.* **2004**, *10*, 1469.
6. Nordberg, A. *Curr. Opin. Neurol.* **2007**, *20*, 398.
7. Furumoto, S.; Okamura, N.; Iwata, R.; Yanai, K.; Arai, H.; Kudo, Y. *Curr. Top. Med. Chem.* **2007**, *7*, 1773.
8. Cai, L. S.; Innis, R. B.; Pike, V. W. *Curr. Med. Chem.* **2007**, *14*, 19.
9. Small, G. W.; Kepe, V.; Ercoli, L. M.; Siddarth, P.; Bookheimer, S. Y.; Miller, K. J.; Lavretsky, H.; Burggren, A. C.; Cole, G. M.; Vinters, H. V.; Thompson, P. M.; Huang, S. C.; Satyamurthy, N.; Phelps, M. E.; Barrio, J. R. *N. Engl. J. Med.* **2006**, *355*, 2652.
10. Shoghi-Jadid, K.; Small, G. W.; Agdeppa, E. D.; Kepe, V.; Ercoli, L. M.; Siddarth, P.; Read, S.; Satyamurthy, N.; Petric, A.; Huang, S. C.; Barrio, J. R. *Am. J. Geriatr. Psychiat.* **2002**, *10*, 24.
11. Agdeppa, E. D.; Kepe, V.; Liu, J.; Flores-Torres, S.; Satyamurthy, N.; Petric, A.; Cole, G. M.; Small, G. W.; Huang, S. C.; Barrio, J. R. *J. Neurosci.* **2001**, *21*, RC189.
12. Klunk, W. E.; Engler, H.; Nordberg, A.; Wang, Y.; Blomqvist, G.; Holt, D. P.; Bergstrom, M.; Savitcheva, I.; Huang, G. F.; Estrada, S.; Ausen, B.; Debnath, M. L.; Barletta, J.; Price, J. C.; Sandell, J.; Lopresti, B. J.; Wall, A.; Koivisto, P.; Antoni, G.; Mathis, C. A.; Langstrom, B. *Ann. Neurol.* **2004**, *55*, 306.
13. Mathis, C. A.; Wang, Y.; Holt, D. P.; Huang, G. F.; Debnath, M. L.; Klunk, W. E. *J. Med. Chem.* **2003**, *46*, 2740.
14. Verhoeff, N. P.; Wilson, A. A.; Takeshita, S.; Trop, L.; Hussey, D.; Singh, K.; Kung, H. F.; Kung, M. P.; Houle, S. *Am. J. Geriatr. Psychiatry* **2004**, *12*, 584.
15. Ono, M.; Wilson, A.; Nobrega, J.; Westaway, D.; Verhoeff, P.; Zhuang, Z. P.; Kung, M. P.; Kung, H. F. *Nucl. Med. Biol.* **2003**, *30*, 565.
16. Kudo, Y.; Okamura, N.; Furumoto, S.; Tashiro, M.; Furukawa, K.; Maruyama, M.; Itoh, M.; Iwata, R.; Yanai, K.; Arai, H. *J. Nucl. Med.* **2007**, *48*, 553.
17. Rowe, C. C.; Ackerman, U.; Browne, W.; Mulligan, R.; Pike, K. L.; O'Keefe, G.; Tochon-Danguy, H.; Chan, G.; Berlangieri, S. U.; Jones, G.; Dickinson-Rowe, K. L.; Kung, H. F.; Zhang, W.; Kung, M. P.; Skovronsky, D.; Dyrks, T.; Holl, G.; Krause, S.; Friebe, M.; Lehman, L.; Lindemann, S.; Dinkelborg, L. M.; Masters, C. L.; Villemagne, V. L. *Lancet Neurol.* **2008**, *7*, 129.
18. Zhuang, Z. P.; Kung, M. P.; Hou, C.; Skovronsky, D. M.; Gur, T. L.; Plossl, K.; Trojanowski, J. Q.; Lee, V. M. Y.; Kung, H. F. *J. Med. Chem.* **2001**, *44*, 1905.
19. Zhuang, Z. P.; Kung, M. P.; Hou, C.; Plossl, K.; Skovronsky, D.; Gur, T. L.; Trojanowski, J. Q.; Lee, V. M. Y.; Kung, H. F. *Nucl. Med. Biol.* **2001**, *28*, 887.
20. Lee, C. W.; Kung, M. P.; Hou, C.; Kung, H. F. *Nucl. Med. Biol.* **2003**, *30*, 573.
21. Kung, M. P.; Hou, C.; Zhuang, Z. P.; Zhang, B.; Skovronsky, D.; Trojanowski, J. Q.; Lee, V. M.; Kung, H. F. *Brain Res.* **2002**, *956*, 202.
22. Zhuang, Z. P.; Kung, M. P.; Wilson, A.; Lee, C. W.; Plossl, K.; Hou, C.; Holtzman, D. M.; Kung, H. F. *J. Med. Chem.* **2003**, *46*, 237.
23. Newberg, A. B.; Wintering, N. A.; Plossl, K.; Hochold, J.; Stabin, M. G.; Watson, M.; Skovronsky, D.; Clark, C. M.; Kung, M. P.; Kung, H. F. *J. Nucl. Med.* **2006**, *47*, 748.
24. Nesterov, E. E.; Skoch, J.; Hyman, B. T.; Klunk, W. E.; Bacskai, B. J.; Swager, T. M. *Angew. Chem.* **2005**, *117*, 5588.
25. Herland, A.; Nilsson, K. P. R.; Olsson, J. D. M.; Hammarstrom, P.; Konradsson, P.; Inganas, O. *J. Am. Chem. Soc.* **2005**, *127*, 2317.
26. Åslund, A.; Herland, A.; Hammarstrom, P.; Nilsson, K. P. R.; Jonsson, B.-H.; Inganas, O.; Konradsson, P. *Bioconjugate Chem.* **2007**, *18*, 1860.
27. Nilsson, K. P. R.; Åslund, A.; Berg, I.; Nystrom, S.; Konradsson, P.; Herland, A.; Inganas, O.; Stabo-Eeg, F.; Lindgren, M.; Westermark, G. T.; Lannfelt, L.; Nilsson, L. N. G.; Hammarstrom, P. *ACS Chem. Biol.* **2007**, *2*, 553.
28. Åslund, A.; Sigurdson, C. J.; Klingstedt, T.; Grathwohl, S.; Bolmont, T.; Dickstein, D. L.; Glimsdal, E.; Prokop, S.; Lindgren, M.; Konradsson, P.; Holtzman, D. M.; Hof, P. R.; Heppner, F. L.; Gandy, S.; Jucker, M.; Aguzzi, A.; Hammarstrom, P.; Nilsson, K. P. R. *ACS Chem. Biol.* **2009**, *4*, 673.
29. Zheng, M. Q.; Yin, D. Z.; Qiao, J. P.; Zhang, L.; Wang, Y. X. *J. Fluorine Chem.* **2008**, *129*, 210.
30. Raposoa, M. M.; Kirschb, G. *Tetrahedron* **2003**, *59*, 4891.
31. Klunk, W. E.; Debnath, M. L.; Pettegrew, J. W. *Biol. Psychiat.* **1994**, *35*, 627.
32. Chun, Y. S.; Lim, S. J.; Oh, S. J.; Moon, D. H.; Kim, D. J.; Cho, C. G.; Yoo, K. H. *Bull. Korean Chem. Soc.* **2008**, *29*, 1765.
33. Goodman, M. M.; Kirsch, G.; Knapp, F. F. *J. Heterocycl. Chem.* **1984**, *21*, 1579.
34. Brown, J. *Endocrinology* **1956**, *58*, 68.
35. Brown, G. K. *Physiol. Rev.* **1961**, *41*, 189.
36. Leder, O. *Histochemistry* **1982**, *74*, 585.
37. Cheng, Y.; Prusoff, W. *Biochem. Pharmacol.* **1973**, *1973*, 3099.
38. Wu, C. Y.; Wei, J. J.; Gao, K. Q.; Wang, Y. M. *Bioorg. Med. Chem.* **2007**, *15*, 2789.